Cancer Letters 507 (2021) 1–12

Contents lists available at ScienceDirect

Cancer Letters

journal homepage: www.elsevier.com/locate/canlet

MMP1 drives tumor progression in large cell carcinoma of the lung through fibroblast senescence

Marta Gabasa [a], Evette S. Radisky [b], Rafael Ikemori [a], Giulia Bertolini [c], Marselina Arshakyan [a], Alexandra Hockla [b], Paula Duch [a], Ornella Rondinone [c], Alejandro Llorente [a], Maria Maqueda [d], Albert Davalos [e], Elena Gavilán [f], Alexandre Perera [d], Josep Ramírez [g,h,i], Pere Gascón [j,k], Noemí Reguart [i,j], Luca Roz [c], Derek C. Radisky [b,**], Jordi Alcaraz [a,h,i,l,*]

[a] Unit of Biophysics and Bioengineering, Department of Biomedicine, School of Medicine and Health Sciences, Universitat de Barcelona, Barcelona, 08036, Spain
[b] Department of Cancer Biology, Mayo Clinic, Jacksonville, FL, 32224, USA
[c] Tumor Genomics Unit, Department of Research, Fondazione IRCCS Istituto Nazionale dei Tumori, Milano, 20133, Italy
[d] Department of ESAII, Center for Biomedical Engineering Research, Technical University of Catalonia (UPC), CIBER de Bioingeniería, Biomateriales y Nanomedicina (CIBER-BBN), Barcelona, 08028, Spain
[e] Buck Institute for Age Research, Novato, CA 94945, USA
[f] Cell Dynamics and Signaling Department, Andalusian Molecular Biology and Regenerative Medicine Centre (CABIMER), CSIC, Sevilla, 41092, Spain
[g] Pathology Service, Hospital Clínic de Barcelona, Barcelona, 08036, Spain
[h] Centro de Investigación Biomédica en Red de Enfermedades Respiratorias (CIBERES), Instituto de Salud Carlos III, Madrid, 28029, Spain
[i] Thoracic Oncology Unit, Hospital Clinic Barcelona, Barcelona, 08036, Spain
[j] Institut d'Investigacions Biomèdiques August Pi i Sunyer (IDIBAPS), Barcelona, 08036, Spain
[k] Department of Medicine, University of Barcelona, Barcelona, Spain
[l] Institute for Bioengineering of Catalonia (IBEC), The Barcelona Institute for Science and Technology (BIST), Barcelona, 08028, Spain

ARTICLE INFO

Keywords:
MMP1
Cancer-associated fibroblasts
senescence
TGF-β
lung cancer

ABSTRACT

Large cell carcinoma (LCC) is a rare and aggressive lung cancer subtype with poor prognosis and no targeted therapies. Tumor-associated fibroblasts (TAFs) derived from LCC tumors exhibit premature senescence, and coculture of pulmonary fibroblasts with LCC cell lines selectively induces fibroblast senescence, which in turn drives LCC cell growth and invasion. Here we identify MMP1 as overexpressed specifically in LCC cell lines, and we show that expression of MMP1 by LCC cells is necessary for induction of fibroblast senescence and consequent tumor promotion in both cell culture and mouse models. We also show that MMP1, in combination with TGF-β1, is sufficient to induce fibroblast senescence and consequent LCC promotion. Furthermore, we implicate PAR-1 and oxidative stress in MMP1/TGF-β1-induced TAF senescence. Our results establish an entirely new role for MMP1 in cancer, and support a novel therapeutic strategy in LCC based on targeting senescent TAFs.

1. Introduction

Lung cancer is the leading cause of cancer-related deaths worldwide, and is histologically classified into non-small cell lung cancer (NSCLC) and small cell lung cancer (SCLC); NSCLC is further subdivided into adenocarcinoma (ADC), squamous cell carcinoma (SCC), and other less frequent subtypes such as large cell carcinoma (LCC) [1,2]. Although all these lung cancer subtypes are epithelial in origin, it is clear that the aberrant stroma that surrounds cancer cells is a key driver of tumor progression [3]. NSCLC stroma is desmoplastic and rich in tumor-associated fibroblasts (TAFs) that exhibit an activated/myofibroblast-like phenotype [4]. Indeed, TAFs are the most abundant stromal cell type, and we and others have reported that TAFs in NSCLC exhibit distinct phenotypic alterations according to the histologic subtype of the tumors from which they are derived [5–7], suggesting that the mechanisms by which TAFs contribute to tumor progression are likely to be cancer subtype-dependent.

Acquisition of a senescent phenotype is emerging as a major tumor-

** Co-Corresponding author. .
* Corresponding author. Unit of Biophysics and Bioengineering, Department of Biomedicine, School of Medicine and Health Sciences, Universitat de Barcelona, Barcelona 08036, Spain
E-mail addresses: Radisky.Derek@mayo.edu (D.C. Radisky), jalcaraz@ub.edu (J. Alcaraz).

https://doi.org/10.1016/j.canlet.2021.01.028
Received 20 November 2020; Received in revised form 9 January 2021; Accepted 28 January 2021
Available online 6 March 2021
0304-3835/© 2021 The Authors. Published by Elsevier B.V. This is an open access article under the CC BY-NC-ND license (http://creativecommons.org/licenses/by-nc-nd/4.0/).

promoting process in TAFs. Senescence is a cell state that arises in response to stress in which cells acquire a permanent growth arrest, yet remain metabolically active. Senescent cells can also display an increase in the secretion of pro-inflammatory and other soluble factors known as the senescence-associated secretory phenotype (SASP) [8,9]. Notably, senescent TAFs have been identified in several solid tumors, in which aggressive tumor progression has been linked to the SASP of senescent TAFs [10–15]. In agreement with these previous observations, LCC tumors often show an aggressive tumor phenotype [16], and we previously reported that TAFs isolated from LCC patients are more likely to be senescent [17], suggesting that senescence of LCC-TAFs could be related to the enhanced invasive and proliferative characteristics of LCC tumors [17].

LCC is a rare NSCLC subtype and, unlike ADC or SCC, it lacks targeted therapies and specific molecular markers, and indeed LCC is commonly diagnosed by exclusion of ADC and SCC markers. These limitations have rendered the study of LCC challenging, and our overall understanding of its tumor biology very limited [2,16,18]. We previously showed that pulmonary fibroblasts became senescent upon indirect coculture with LCC cell lines but not with non-LCC cell lines, revealing that LCC cells secrete factors that induce paracrine senescence in fibroblasts. We also showed that senescent pulmonary fibroblasts enhanced the growth and dissemination of LCC cells in culture and *in vivo* compared to control (non-senescent) fibroblasts [17], further implicating fibroblast senescence in the aggressive nature of LCC. However, the identity of factor(s) produced by LCC cells that induce senescence of pulmonary fibroblasts has remained unknown.

The work presented here identifies matrix metalloproteinase-1 (MMP1) as the key LCC-secreted factor underlying paracrine senescence in fibroblasts and consequent enhancement of tumor-promoting traits. These results establish an entirely new role for MMP1 in cancer, in contrast with its well-known function of proteolytic degradation of fibrillar collagens [19,20], and define a new paradigm for MMP1-dependent paracrine activation of protumorigenic senescent fibroblasts in LCC progression. Moreover, we identify a new therapeutic strategy for this poorly understood cancer type based on targeting senescent fibroblasts.

2. Materials and methods

2.1. Cell culture

The normal pulmonary fibroblast cell line CCD-19Lu (ATCC) was maintained as described [17]. Unless otherwise indicated, fibroblasts were seeded as 5.2×10^3 cells/cm^2 collagen-coated culture plates [17]. In some experiments, CCD-19Lu fibroblasts were exposed to 45U/ml rMMP1, 2.5 ng/ml recombinant human TGF-β1 (R&D Systems), or both in the presence or absence of 4 mM n-acetyl cysteine (NAC) (Sigma) for 7 days. A randomly selected panel of NSCLC cell lines derived from LCC (H460, H1299 and H661) or non-LCC patients (H1437, H358, H1703, A549 and H23) (ATCC) was used in coculture experiments and/or microarray expression analysis (Supplementary Table 1). Cancer cells were cultured as described [17,21]. Primary mouse skin fibroblasts were obtained from tissue explants as reported [17]. Cells were routinely tested for mycoplasma contamination.

2.2. Recombinant protein production

The proMMP1 catalytic domain expression construct was a generous gift from H. Nagase [22]. ProMMP1 catalytic domain was expressed, refolded, and purified [23], and proteolytically activated to produce the active MMP1 catalytic domain (rMMP1).

2.3. Knock-down of MMP1 and PAR-1

MMP1 was stably knocked-down in LCC cancer cells with two lentiviral shRNA contructs (shMMP1 #1 and #2), and a non-target Scramble control (Scr) shRNA was used as a control as described [24]. PAR-1 was transiently knocked-down in control fibroblasts by siRNA.

2.4. Measurement of MMP activity in conditioned media

Culture media of parental and MMP1-knocked down LCC cells were collected and assayed for MMP activity using an MMP colorimetric substrate assay (EnzoLife Sciences).

2.5. Heterotypic coculture of cancer cells and fibroblasts

Transwells were used as described [17]. CCD-19Lu fibroblasts were seeded in the collagen-coated bottom Transwell plate, and cancer cells were seeded on the Transwell insert at 2.2×10^4 cells/cm^2 in serum-free medium for 9 days. Bare (cell-free) inserts were used as controls. For flow cytometry experiments, cocultures were conducted in duplicates and, after 9 days, were stimulated with 10% FBS or 0% FBS for 24 h. For rescue experiments, 45 U/ml rMMP1 was added to the cocultures in every medium change (2–3 days).

2.6. Conditioned medium (CM) of fibroblasts

Fibroblasts were maintained for 4 additional days in serum-free fibroblast culture medium following coculture (upon removing the Transwell insert) or stimulation with rMMP1, TGF-β1 or both. The CM was centrifuged and stored until use [17].

2.7. Senescence-associated beta-galactosidase (SA-βgal)

SA-βgal activity was detected as described [17]. For each experiment, the average percentage of SA-βgal+ cells under basal (control) conditions SA-βgal+ were substracted.

2.8. qRT-PCR

RNA extraction and reverse transcription were conducted as reported [6].

2.9. Flow cytometry

Cell cycle analysis was performed as reported [17].

2.10. Western blot

Western blot analysis of p16^{INK4a} and PAR-1 was performed as reported [6].

2.11. TGF-β activity reporter assay

The activity of bioactive TGF-β was monitored using the TGF-β-inducible p(CAGA)$_{12}$ luciferase-reporter as described [6,25].

2.12. Cancer cell growth and invasion

The effect of the CM on cancer cell growth and invasion was assessed as described [17]. In brief, to assess cancer cell growth, cancer cells were stimulated with CM for 3 days, and their nuclei were fluorescently stained and counted to measure cell density as the average nuclear density/image. To assess cell invasion we used the Matrigel Transwell invasion assay, in which CM was added to the lower Transwell compartment, and cancer cells that invaded the Matrigel layer through the other side of the Transwell porous membrane were stained with crystal violet and quantified as positive crystal violet staining area/image.

2.13. In vivo tumorigenicity and tumor dissemination

In vivo tumorigenic assays were carried out as reported [17], using protocols approved by the Ethics Committee of the Fondazione IRCCS INT according to EU Directive 2010/63/EU. Scramble control or shMMP1 H460 cells (1×10^3) were diluted 1:1 with 0.1 mL of Cultrex Basement Membrane (Trevigen) and subcutaneously injected into both flanks of CD1-nude female mice (Charles River Laboratories) 8 weeks old (n = 5/cell condition). Tumor growth was monitored for ~25 days by assessing tumor volume [17]. At the end of the observation period or when tumors reached 300 mm^3, mice were euthanized, tumor xenografts were paraffin-embedded for Sentragor staining, and lungs were removed and dissociated to assess tumor dissemination by flow cytometry [17].

2.14. Histologic analysis

Fibroblast senescence assessment through biotin-linked sudan black B analogue (Sentragor) staining was conducted following manufacturers' instructions [26]. Quantitative image analysis was carried out with ImageJ [27] under the guidance of our pathologist (JR). Fibroblasts were identified through their spindle-shaped nuclei as reported [5,28].

2.15. Transcriptional analysis of selected cell lines

Cell line selection and culture conditions, sample preparation, gene expression experiments, and data normalization and processing are described elsewhere [21]. Transcriptional profiles of randomly selected LCC (H460, H661) and non-LCC (A549, H1437, H358, H1703, and H23) cell lines grown on tissue culture plastic are deposited in the Gene Expression Omnibus (GEO) as GSE158597, and were analyzed to identify 1052 differentially expressed probesets that correspond to 678 annotated genes (Supplementary Table 2).

2.16. Gene expression analysis of cell lines with public databases

The expression of *MMP1* and *TGFB1* was analyzed in an extended panel of LCC (n = 10) and non-LCC (7 ADC, 4 SCC) cell lines (Supplementary Table 1) using publicly available datasets in R [29].

2.17. Statistical analysis

Two group comparisons were performed with two-tailed Student *t*-test (SigmaPlot). Statistical significance was assumed at $P < 0.05$, whereas $P < 0.1$ was interpreted as marginally significant. All experiments were conducted as triplicates. The percentages of tumor-free mice were compared with log-rank test (GraphPad Prism v5.0.). All data shown are mean ± s.e.m.

Further details on the methods and additional methodology are included in Supplementary Material.

3. Results

3.1. MMP1 is selectively overexpressed in LCC cell lines, and is necessary for the paracrine induction of fibroblast senescence

To identify the factor(s) secreted by LCC cells that induce senescence of cocultured fibroblasts, we evaluated gene expression differences between a randomly selected panel of cultured LCC (H460, H661) and non-LCC cell lines (i.e. ADC and SCC: H1437, H358, H1703, A549 and H23). Hierarchical gene clustering revealed similarities between LCC lines and differences from non-LCC lines, and identified 678 differentially expressed genes in LCC as compared to non-LCC (Fig. 1A). Subsequent KEGG-based pathway enrichment analysis reported 22 statistically significant over-represented pathways, among which *KEGG Pathways in cancer* was the largest with 23 genes (Fig. 1B, Supplementary Table 3). Within the latter 23 genes, the largest LCC-upregulated gene coding for a secreted factor was *MMP1* (Supplementary Table 4). *MMP1* overexpression in H460 and H661 LCC cells was confirmed by qRT-PCR (Supplementary Fig. S1A). Likewise, we examined *MMP1* expression in an extended cell line panel using the Sanger database (Supplementary Table 1) and found that it was upregulated in LCC cell lines compared to non-LCC cell lines (Fig. 1C); consistent results were obtained with the CCLE database (Supplementary Fig. S1B).

To assess whether expression of *MMP1* by LCC cells was required for induction of senescence in cocultured fibroblasts, we knocked-down *MMP1* expression in three LCC cell lines (H460, H1299 and H661) by shRNA using two different plasmids, whereas shScramble (Scr) was used as a control (Fig. 1D and E, Supplementary Fig. S1C), and analyzed three standard senescence markers: induction of senescence-associated beta-galactosidase (SA-βgal), permanent growth arrest, and expression of cell cycle inhibitor *CDKN2A* ($p16^{INK4a}$) in fibroblasts cocultured with LCC lines with reduced *MMP1* expression (Fig. 1F). Knocking-down *MMP1* did not affect proliferation of LCC cells (Supplementary Fig. S1D), but did significantly reduce both the specific MMP activity in the conditioned medium of LCC cells (Supplementary Fig. S1E) and their ability to induce senescence of cocultured fibroblasts as assessed by SA-βgal (Fig. 1G and H). Consistently, fibroblasts cocultured with knocked-down *MMP1* LCC cells (H460, H1299) exhibited a marked drop in the percentage of G0/G1 arrested cells upon stimulation with 10% FBS compared to serum-free medium (0% FBS), indicating that they re-entered proliferation with serum stimulation; in contrast, fibroblasts cocultured with Scr LCC cells maintained G0/G1 arrest in agreement with a senescent phenotype (Fig. 1I and J, Supplementary Fig. S1F). Likewise, a marked drop in *CDKN2A* mRNA and corresponding $p16^{INK4a}$ protein expression was observed in fibroblasts cocultured with knocked-down *MMP1* H460 cells upon 10% FBS with respect to 0% FBS (Fig. 1K and L), whereas such drop was significantly attenuated in fibroblasts cocultured with Scr cells. Consistent results were obtained upon coculture with the LCC cell line H661 (Supplementary Fig. S1G). These findings show that expression of *MMP1* in LCC cells is responsible for paracrine induction of fibroblast senescence.

3.2. MMP1 knock-down in LCC cells abrogates the tumor-promoting effects of cocultured fibroblasts in culture, and impairs tumor growth in vivo

We previously showed that conditioned medium (CM) from fibroblasts cocultured with LCC cell lines enhanced growth and invasion of these LCC cells [17]. Here we found that this effect was strongly attenuated when using CM from fibroblasts cocultured with shMMP1 LCC cells (H460, H1299) (Fig. 2A–D), and similar results were found in cocultures with H661 cells (Supplementary Figs. S2A and S2B). The cytokines *IL6* and *IL8* are considered key elements of the secretome of senescent cells or SASP [8], and were significantly upregulated in fibroblasts cocultured with H460 and H1299 cells infected with control (Scr) lentivirus at the mRNA level and as a secreted protein (Fig. 2E–H, Supplementary Fig. S2C), in agreement with a senescent phenotype. However, this upregulation was markedly attenuated with the knock-down of MMP1 for H460 cells (Fig. 2E and G; Supplementary Fig. S2C) but only modestly in H1299 (Fig. 2F and H) or H661 cell lines (Supplementary Figs. S2D and S2E), suggesting that the enhanced tumor-promoting traits of senescent fibroblasts through coculture with MMP1-expressing LCC cells is associated with SASP factors other than *IL6* and *IL8*.

To assess the effects of MMP1 knock-down *in vivo*, we injected either control (shScr) or shMMP1 H460 cells subcutaneously into the flanks of immunodeficient CD-1 nude mice (Fig. 3A). We first confirmed that control H460 cells in cocultures do induce senescence of primary skin fibroblasts derived from adult mice, and that this induction was significantly attenuated in cocultures with shMMP1 H460 cells (Fig. 3B). Next, we confirmed that *MMP1* mRNA of LCC cells remained

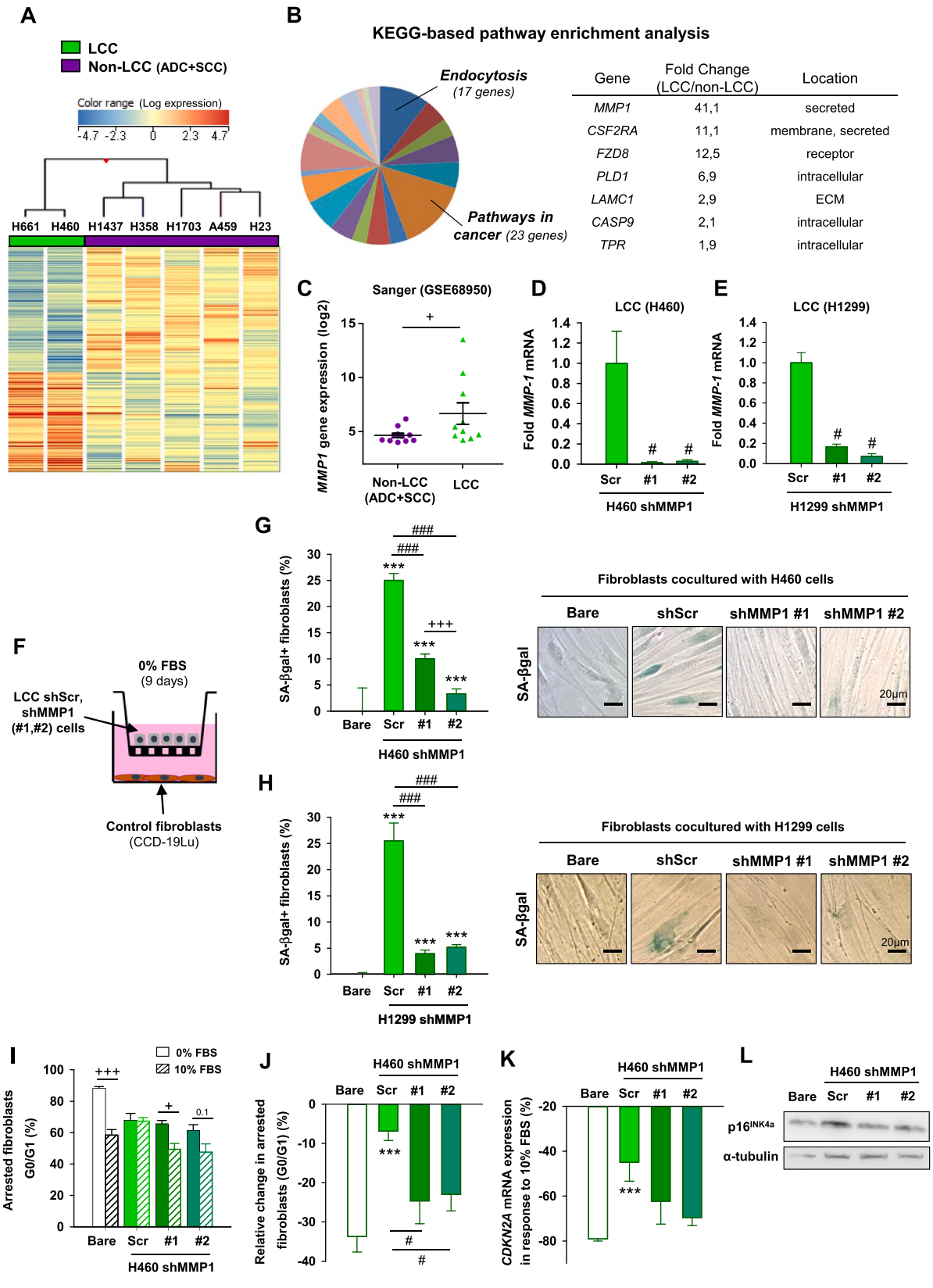

* $P < 0.05$; ** $P < 0.01$; *** $P < 0.005$ comparing to Bare
\# $P < 0.05$; ## $P < 0.01$; ### $P < 0.005$ comparing to Scr
\+ $P < 0.05$; ++ $P < 0.01$; +++ $P < 0.005$ in all other relevant pairwise comparisons

(caption on next page)

Fig. 1. *MMP1* overexpression in LCC cells and its role in the paracrine induction of fibroblast senescence. **A,** Hierarchical clustering of 1052 differentially expressed probesets between a subset of LCC and non-LCC cell lines. **B,** KEGG-based pathway enrichment analysis identified *Pathways in Cancer* as the largest over-represented pathway (Supplementary Table 3), in which *MMP1* was the single gene coding for a secreted factor within the top 5 LCC-upregulated genes. **C,** *MMP1* mRNA expression from the Sanger dataset in an extended panel of cancer cell lines. **D and E,** *MMP1* expression in H460 (D) and H1299 (E) LCC cell lines after *MMP1* knockdown by shRNA using two plasmids (#1, #2) and shScramble (Scr) as a control. **F,** Outline of the LCC cell-fibroblast cocultures with transwells. **G and H,** Percentage of SA-βgal+ fibroblasts upon coculture with shMMP1 H460 (G) or H1299 (H) LCC cells as in (F). Representative SA-βgal images shown to the right. **I and J,** Percentage of growth arrested fibroblasts (I) cocultured with H460 cells as in (F), and corresponding relative change (J). **K and L,** Relative change in the *CDKN2A* ($p16^{INK4a}$) mRNA (K) or protein (L) expression of fibroblasts cocultured as in (J). Similar results were obtained with H1299 (Supplementary Fig. S1E) and H661 (Supplementary Fig. S1F) cells. Error bars indicate mean ± s.e.m. *, $P < 0.05$; **, $P < 0.01$; ***, $P < 0.005$ comparing to Bare conditions. #, $P < 0.05$; ##, $P < 0.01$; ###, $P < 0.005$ comparing to Scr. + $P < 0.05$; ++ $P < 0.01$; +++ $P < 0.005$ in all other relevant pairwise comparisons. All comparisons were done using Student *t*-test. Mean values correspond to n = 4 experiments (D-K).

significantly downregulated in tumor xenografts bearing MMP1 knocked-down H460 cells compared to parental cells at the end of the observation period using human specific primers (Fig. 3C). In agreement with our *in vitro* findings, we found a significant reduction of tumor growth (Fig. 3D) and tumor take (Fig. 3E) in tumors bearing shMMP1 cells compared to parental cells. We also observed that tumors from shMMP1 H460 cells exhibited fewer senescent fibroblasts compared to control H460 cells, as indicated by the significant drop in the percentage of fibroblasts positively stained with biotin-linked sudan black B (Sentragor) (Fig. 3F), which detects senescent cells in paraffin-embedded tissue [8]. Notably, tumors from shMMP1 H460 cells also exhibited significantly fewer lung disseminated tumor cells (DTC) (Fig. 3G) compared to control H460 cells. Collectively, these observations strongly support that *MMP1* in LCC cells is necessary for the aberrant accumulation of tumor-promoting senescent fibroblasts.

3.3. Recombinant MMP1 (rMMP1) partially rescues fibroblast senescence and their enhanced tumor-promoting traits in cocultures

We next assessed whether MMP1 was sufficient to induce fibroblast senescence and/or to enhance the tumor-promoting traits of the senescent fibroblast secretome. Exposure of control fibroblasts with 45 U/ml active rMMP1 for 7 days did not significantly increase the proportion of SA-βgal + fibroblasts (Fig. 4A) or the mRNA expression of SASP markers *IL6* and *IL8* (Fig. 4B and C). Consistently, the CM of fibroblasts treated with rMMP1 alone did not increase the growth and invasion of H460 (Fig. 4D and F) or H1299 (Fig. 4E and G) LCC cells, and even decreased invasion in H460, although modestly. However, addition of 45 U/ml rMMP1 to the media of control fibroblasts cocultured with either shMMP1 H460 or H1299 cells (Fig. 4H) significantly increased SA-βgal positivity (Fig. 4I and J). Consistent results were obtained with H661 LCC cells (Supplementary Fig. S3). Supplementation with rMMP1 also rescued the ability of shMMP1 H460 or H1299 to induce the growth and invasion-promoting effect of the CM of cocultured fibroblasts (Fig. 4K-N), although with marginal significance in terms of growth. These results reveal that rMMP1 alone is not sufficient to induce fibroblast senescence or enhance the tumor-promoting traits of their CM, and supports that it requires cofactor(s).

3.4. Combining rMMP1 and TGF-β1 is sufficient to induce fibroblast senescence and consequent tumor-promoting effects

Because TAFs from LCC patients exhibit an activated/myofibroblast-like phenotype [17], and TGF-β1 is a known fibroblast activator [30] that is frequently upregulated in NSCLC [31] and has been implicated in senescence [8], we examined the effects of combining rMMP1 with TGF-β1 on control pulmonary fibroblasts. While exposure to either rMMP1 or TGF-β1 alone did not increase the percentage of SA-βgal+ fibroblasts, combining both factors did, eliciting percentages comparable to the average percentage attained upon coculture with our panel of LCC cells (Fig. 5A). Likewise, the CM of fibroblasts co-stimulated with rMMP1 and TGF-β1 significantly enhaced the growth (Fig. 5B and C) and invasion (Fig. 5D and E) of both H460 and H1299 cells up to levels comparable to those attained with the CM of senescent fibroblasts cocultured with parental cells. In agreement with previous findings [28], we also observed that the CM of fibroblasts stimulated with TGF-β1 alone increased the growth of both H460 (Fig. 5B) and H1299 (Fig. 5C) cells, although up to levels that were ~10% and ~25% lower than those attained in combination with rMMP1, respectively; however, CM of fibroblasts treated with TGF-β1 alone did not significantly increase invasion of cocultured LCC cells (Fig. 5D and E). These observations reveal a novel interaction between MMP1 and TGF-β1 that elicits fibroblast senescence concomitantly with an enhancement of the tumor-promoting traits of their secretome on LCC cells.

To further implicate TGF-β1 in LCC-induced fibroblast senescence, we first examined *TGFB1* mRNA in an extended panel of cell lines in the Sanger database (Supplementary Table 1), and found a significant upregulation in LCC compared to non-LCC lines (Fig. 5F). Next, we examined the bioactivity of secreted TGF-β1 in coculture experiments using the CAGA reporter, and found a significant increase in fibroblasts cocultured with H460 LCC cells compared to bare control (Fig. 5G), concomitantly with an increase in the expression of fibroblast activation markers *COL1A1* (Fig. 5H) and α-SMA (Supplementary Fig. S4). These results strongly support the presence of an aberrantly large TGF-β1 expression selectively in LCC cells.

3.5. Oxidative stress and F2R (PAR-1) are implicated in the pro-senescence and tumor-promoting effects elicited by rMMP1 and TGF-β1 in fibroblasts

To begin to unravel the mechanisms underlying fibroblast senescence elicited by co-stimulation with rMMP1 and TGF-β1, we used three complementary strategies. First, we examined autophagy, a cellular recycling process that becomes upregulated under some types of stress, since it frequently increases during senescence [8], and previous work linked autophagy and senescence in breast cancer TAFs [11]. However, the expression of the canonical autophagy marker LC3B did not increase in fibroblasts with *induced* senescence upon coculture with H460 cells (Supplementary Figs. S5A–D), thereby discounting an important role of autophagy in LCC-induced fibroblast senescence.

Next we examined the role of oxidative stress, since we previously reported that the antioxidant n-acetyl cysteine (NAC) dose-dependently reduced the percentage of SA-βgal+ fibroblasts in cocultures with H460 cells [17]. We first confirmed that NAC attenuated fibroblast senescence upon coculture with H460 in terms of SA-βgal+ cells (Fig. 6A) and expression of SASP factors *IL6* and *IL8* (Fig. 6B and C). Furthermore, we found that NAC significantly attenuated the increase in SA-βgal+ fibroblasts elicited by co-stimulation with rMMP1 and TGF-β1 (Fig. 6D), and the corresponding CM elicited a significantly lower growth (Fig. 6E) and invasion (Fig. 6F) of H460 cells, implicating oxidative stress in both LCC-induced fibroblast senescence and the consequent activation of their tumor-promoting secretome.

Finally, we analyzed the role of the protease-activated receptor PAR-1, which is a G protein–coupled receptor previously involved in transducing signals downstream of MMP1 in stromal cells that is coded by the *F2R* gene [32]. Intriguingly, inducing fibroblast senescence through either co-stimulation with rMMP1 and TGF-β1 or coculture with H460 cells consistently downregulated *F2R* (PAR-1) mRNA (Fig. 6G) and

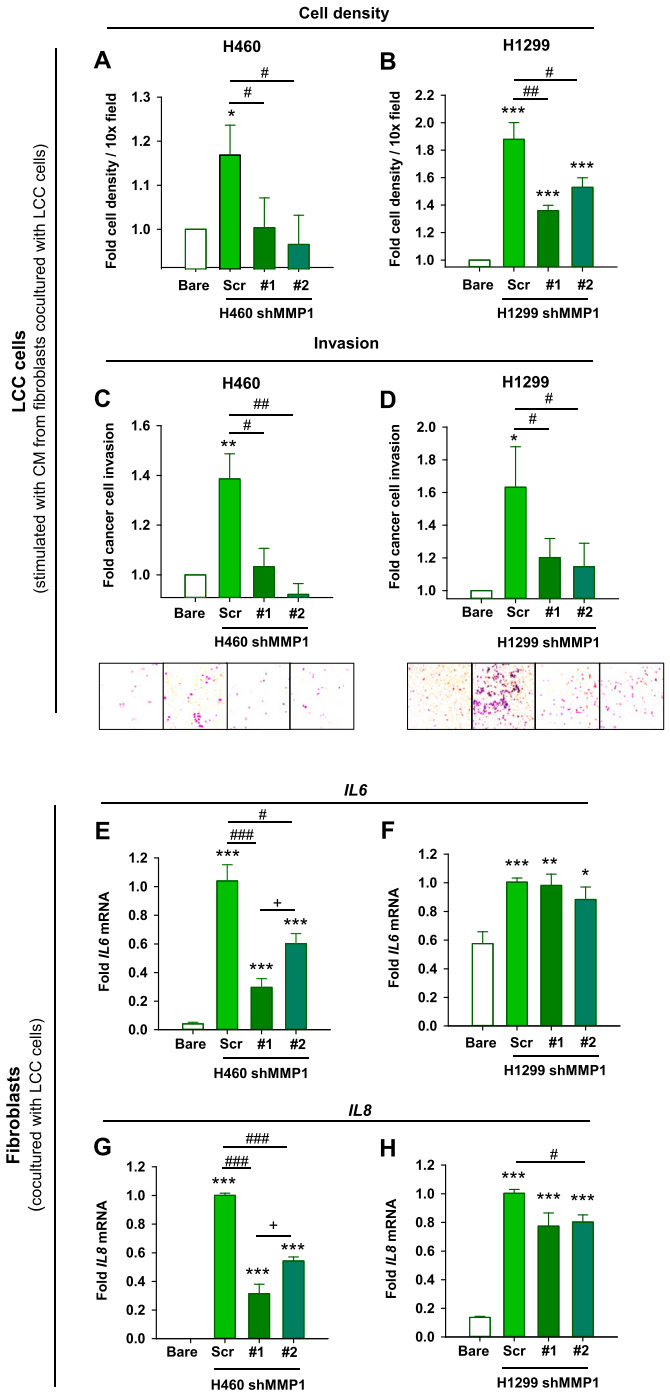

Fig. 2. Role of MMP1 in LCC cells in the tumor-promoting effects of cancer-educated fibroblasts in culture. **A and B,** Fold cell number density of H460 (A) and H1299 (B) cells stimulated with the CM of fibroblasts cocultured alone (Bare), shScr (Scr) or shMMP1 LCC cells as in Fig. 1F. CM was obtained from fibroblasts kept in serum-free medium for 4 days after coculture here and thereafter. **C and D,** Fold invasion of H460 (C) and H1299 (D) LCC cells stimulated with the same CM as in (A) and (B). Representative images of invading cells are shown at the bottom. **E-H,** Fold mRNA expression of SASP factors *IL6* (E and F) and *IL8* (G and H) of fibroblasts cocultured with H460 and H1299 as in Fig. 1E and G, respectively. Similar results were obtained with H661 cells (Supplementary Figs. S2A–D). Statistical analysis as in Fig. 1. Error bars represent mean ± s.e.m. Mean values correspond to n = 4 experiments.

corresponding protein expression (Fig. 6H), whereas such downregulation was abrogated upon coculture with shMMP1 H460 cells (Fig. 6I). Likewise, forcing *F2R* downregulation in control fibroblasts by siRNA (Fig. 6J, Supplementary Fig. S5E) elicited a similar increase in SA-βgal+ fibroblasts upon coculture with H460 cells compared to siControl (Fig. 6K), and even a larger expression of senescence markers *IL6* and *IL8* (Fig. 6L and M) suggestive of a stronger senescent phenotype. These results strongly support that the *F2R* downregulation elicited downstream of rMMP1 and TGF-β1 may be involved in their induction of fibroblast senescence. All these mechanistic insights are summarized in Fig. 6N.

4. Discussion

MMPs have been long appreciated as important mediators of tissue remodeling, targeting for proteolysis numerous extracellular matrix components. MMPs are also dysregulated in cancer [33], where they facilitate tumor progression [34,35]. MMP1 overexpression is a marker of tumor progression and metastasis in a variety of cancer types including lung cancer [19,20], and knocking-out *Mmp1a*, the murine ortholog of human *MMP1*, was sufficient to reduce lung carcinomas induced by a chemical carcinogen in mice [20]. Yet, our understanding of how MMP1 contributes to tumor progression has been very limited, and largely associated to its ability to degrade fibrillar collagens and, more recently, to regulate Th1/Th2 inflammatory responses [19,20]. Here we report a novel tumor-promoting function of MMPs [19,33] by identifying MMP1 production by LCC cells as a key factor in the induction of paracrine senescence in fibroblasts and consequent hyper-activation of their tumor-promoting traits. Importantly, our findings implicate MMP1-induced fibroblast senescence in the aggressive nature of LCC, whose specific tumor biology has remained largely obscure.

Our novel observations provide the first evidence of a causal relationship between MMP1 and senescence, which was unexpected considering previous observations of MMP1 upregulation as a *consequence* rather than a *cause* of senescence [9]. In addition, we found that MMP1 is not sufficient to induce paracrine fibroblast senescence or to enhance their tumor promoting traits, and identified TGF-β1 as a strong candidate co-factor. This observation was also somewhat surprising, since the most well-known effect of TGF-β1 in fibroblasts is to elicit an activated/myofibroblast-like phenotype [36]. Although a previous study on oral squamous TAFs reported that stimulation with TGF-β1 could induce senescence [10], our previous [17] and present work did not identify any evidence of senescence in pulmonary fibroblasts stimulated with TGF-β1 alone [17], suggesting that the ability of TGF-β1 to induce fibroblast senescence may depend on the tissue source of the fibroblasts.

Our results also provide insights on the mechanisms underlying the cooperation between MMP1 and TGF-β1 in eliciting fibroblast senescence and enhancing their tumor-promoting traits, since we identified oxidative stress as a key mediator of both processes. Consistently, oxidative stress has been associated with aggressiveness in LCC [37]. Likewise, our findings are in agreement with the extensive evidence that TGF-β1 increases oxidative stress in fibroblasts [8], and with the limited evidence that MMP1 induces oxidative stress, although indirectly through collagen fragmentation [38]. Furthermore, our results implicate the downregulation of *F2R* (PAR-1), which may be indicative of PAR-1 activation [32], in the aberrant accumulation of senescent TAFs in LCC, since all conditions that induce fibroblast senescence consistently reduced *F2R*, and genetic downregulation of *F2R* elicited a stronger senescent phenotype. However, to our knowledge the role of PAR-1 in fibroblast senescence is unknown, and clarifying its interaction with MMP1 and/or TGF-β1 requires further investigations. In addition, it is conceivable that MMP1 may contribute directly to the increase in TGF-β1 bioactivity, since MMP1 was reported to cleave the latent form of TGF-β [39], and we observed both an increase in TGF-β1 bioactivity in

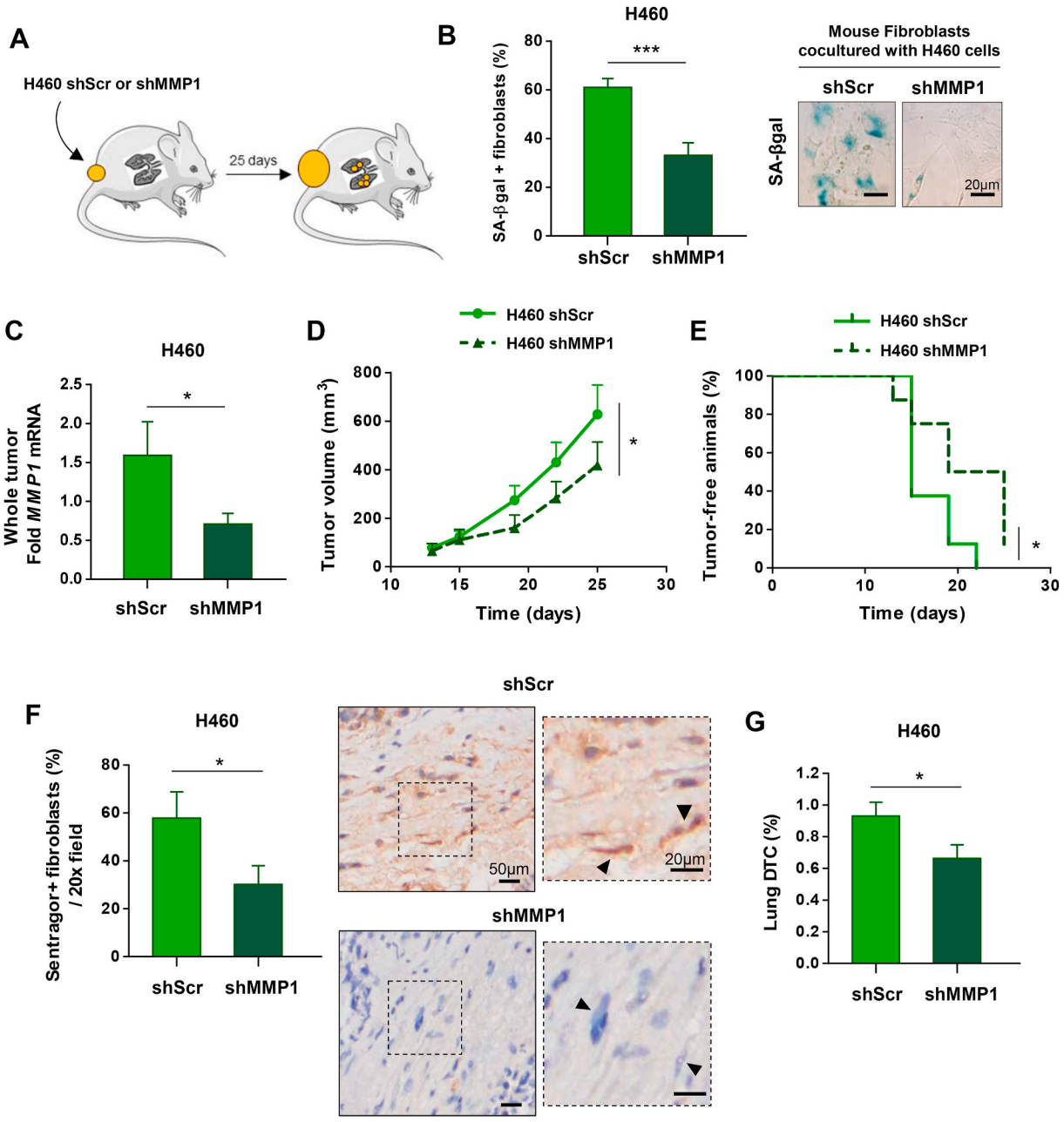

Fig. 3. Role of MMP1 in LCC cells in fibroblast senescence and tumor promotion *in vivo*. **A,** Outline of the experimental design used to assess tumor growth and lung dissemination of H460 LCC cells (shScr or shMMP1) subcutaneously injected into immunodefficient CD-1 mice (n = 5 per condition). **B,** Percentage of SA-βgal+ primary mouse skin fibroblasts upon coculture with control (Scr) or shMMP1 H460 cells. **C,** Fold *MMP1* mRNA expression with respect to a calibrator in tumor xenografts assessed at the end of the observation period. **D,** Average tumor growth. **E,** Percentage of tumor-free flanks (tumors < 150 mm^3). **F and G,** At the end of the observation period, primary tumor xenografts were analyzed to assess the percentage of Sentragor positive fibroblasts (F, representative images of Sentragor staining shown to the right), whereas the lungs were examined to assess the percentage of disseminated tumor cells (DTCs) (G). Arrowheads in (F) point to spindle-shaped nuclei characteristic of fibroblasts. Error bars indicate mean ± s.e.m. Statistical significance in (E) was assessed by log-rank test. All other pairwise comparisons were performed with Student *t*-test. *, $P < 0.05$.

fibroblasts cocultured with LCC cells as well as the rescue of fibroblast senescence and subsequent tumor-promotion of its secretome upon addition of rMMP1 in fibroblasts cocultured with shMMP1 LCC cells. In further agreement with our observed tumor-promoting interaction between MMP1 and TGF-β, previous work reported smaller lung carcinomas in *Mmp1a* knock-out mice exposed to chemical carcinogens compared to parental mice concomitantly with decreased levels of active TGF-β1 [20].

The identification of the specific factors secreted by senescent TAFs that drive LCC growth and metastasis remain to be elucidated. Yet, previous studies have suggested that enhancing cancer cell invasion and dissemination is a predominant tumor-promoting feature of senescent TAFs as part of their complex secretome or SASP [14]. In agreement with this interpretation we found that the secretome of non-senescent and TGF-β1-activated fibroblasts increased LCC growth but not invasion. Moreover, senescent fibroblasts may drive tumor progression further by rendering an immunosuppressive microenvironment through the regulation of immune cell infiltration and activation [40]. Intriguingly, knocking-down MMP1 in a panel of three LCC cell lines consistently abrogated the enhanced tumor-promoting traits of the secretome of

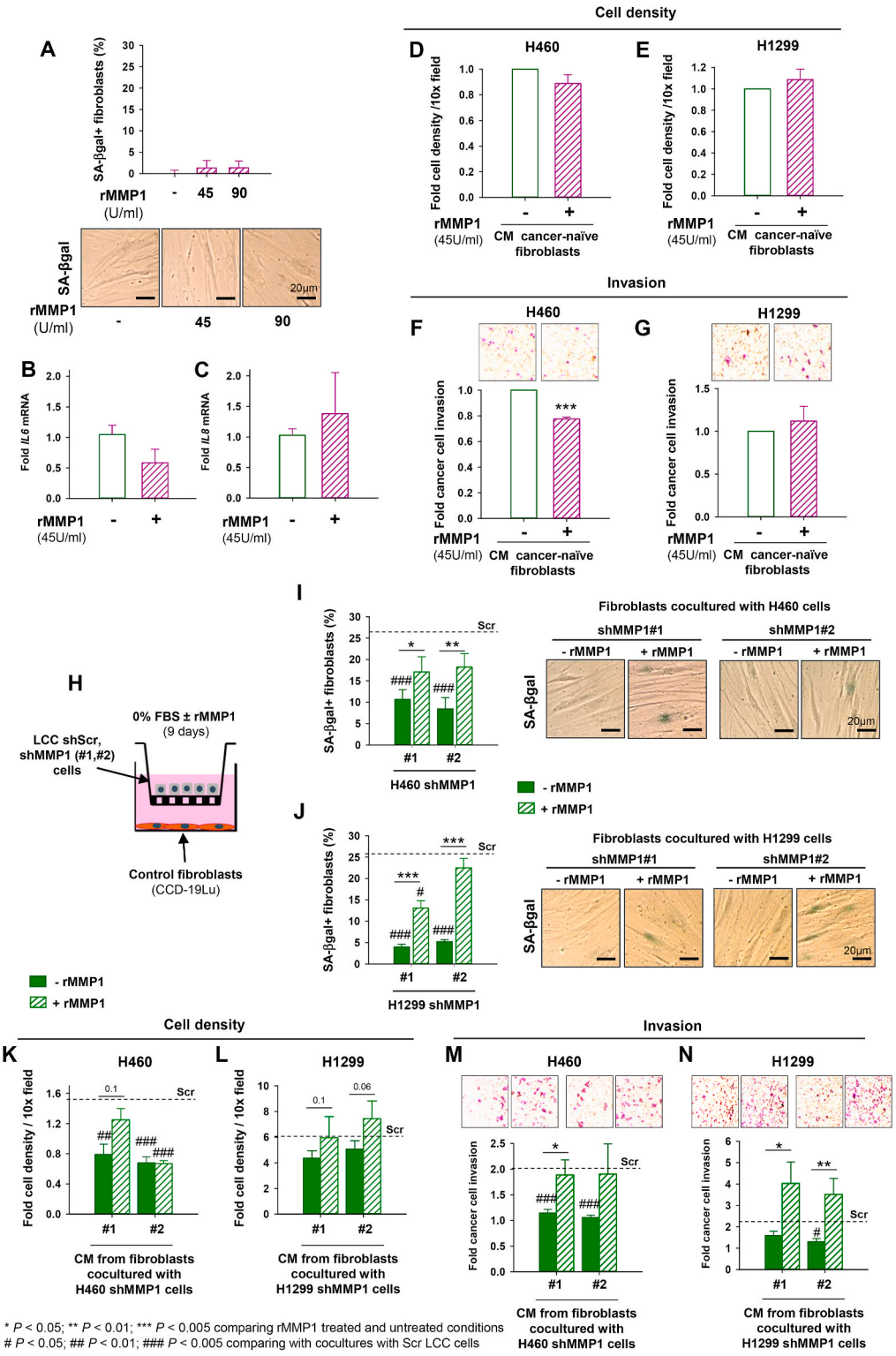

Fig. 4. Recombinant MMP1 (rMMP1) effect on fibroblast senescence and tumor-promoting traits. **A,** Percentage of SA-βgal+ fibroblasts cultured with or without rMMP1 (added every media change) for 7 days. Representative images of SA-βgal staining shown at the bottom. **B and C,** Fold *IL6* (B) and *IL8* (C) mRNA expression of fibroblasts cultured as in (A). **D-G,** Fold cell number density (D and E) and invasion (F and G) of H460 and H1299 LCC cells stimulated with the CM of control fibroblasts cultured as in (A). **H,** Outline of the rescue experimental design, where fibroblasts and shMMP1 LCC cells were cocultured with or without rMMP1. **I and J,** Percentage of SA-βgal+ fibroblasts cocultured as in (H) with H460 (I) or H1299 (J) shMMP1 cells. Corresponding average values obtaind with parental shScr cells are shown as a reference (horizontal line) here and thereafter. Representative images of SA-βgal staining shown to the right. Similar results were obtained with H661 cells (Supplementary Fig. S3). **K-N,** Fold cell number density and invasion of H460 (K and M, respectively) and H1299 (L and N, respectively) stimulated with the CM of fibroblasts cultured as in (H) and subsequently maintained in serum free medium for 4 days. *, $P < 0.05$; **, $P < 0.01$; ***, $P < 0.005$ comparing rMMP1 treated and untreated conditions. #$P < 0.05$; ##, $P < 0.01$; ###, $P < 0.005$ comparing with cocultures with Scr LCC cells. All comparisons were done using Student *t*-test. Mean values correspond to n = 3 experiments.

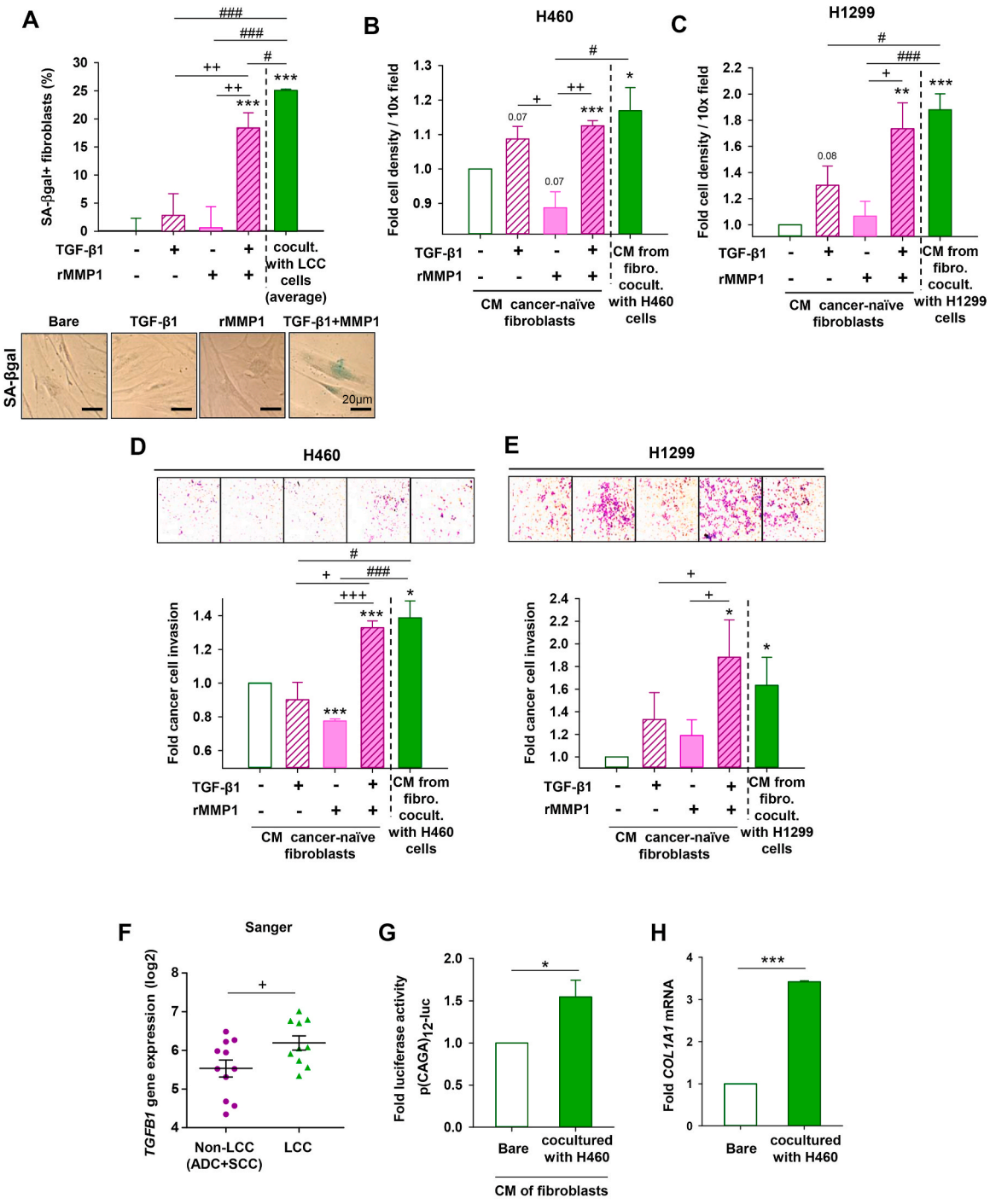

* $P < 0.05$; ** $P < 0.01$; *** $P < 0.005$ comparing to either untreated or Bare conditions
\# $P < 0.05$; ## $P < 0.01$; ### $P < 0.005$ comparing to coculture with LCC cells
\+ $P < 0.05$; ++ $P < 0.01$; +++ $P < 0.005$ in all other pairwise comparisons

Fig. 5. Effect of rMMP1 and TGF-β1 on fibroblast senescence and tumor-promoting traits. **A,** Percentage of SA-βgal+ fibroblasts untreated or treated with 45U/ml rMMP1, 2.5 ng/ml TGF-β1 or both for 7 days. Representative images shown at the bottom. Average percentage of SA-βgal+ fibroblasts cocultured with LCC cancer cells was added as a reference (green bars). **B-E,** Fold cancer cell number density and invasion of H460 (B and D, respectively) and H1299 (C and E, respectively) cells stimulated with the CM of fibroblasts cultured as in (A). Representative images of invading cancer cells are shown above invasion plots. **F,** *TGFB1* mRNA expression from the Sanger dataset in the panel of cancer cell lines used in Fig. 1C. **G,** Bioactivity of the TGF-β1 within the CM of fibroblasts cocultured with H460 or Bare conditions at day 4. **H,** Fold *COL1A1* mRNA expression in fibroblasts cocultured with H460 cells or Bare as in Fig. 1F. Similar results were obtained with H661 cells (Supplementary Fig. S4). *, $P < 0.05$; **, $P < 0.01$; ***, $P < 0.005$ comparing to either untreated or Bare conditions. #, $P < 0.05$; ##, $P < 0.01$; ###, $P < 0.005$ comparing to coculture with LCC cells. + $P < 0.05$; ++ $P < 0.01$; +++ $P < 0.005$ in all other pairwise comparisons. All comparisons were done using Student *t*-test. Error bars represent mean ± s.e.m. Mean values correspond to n = 2 (G and H) and n = 3 experiments (all other). (For interpretation of the references to color in this figure legend, the reader is referred to the Web version of this article.)

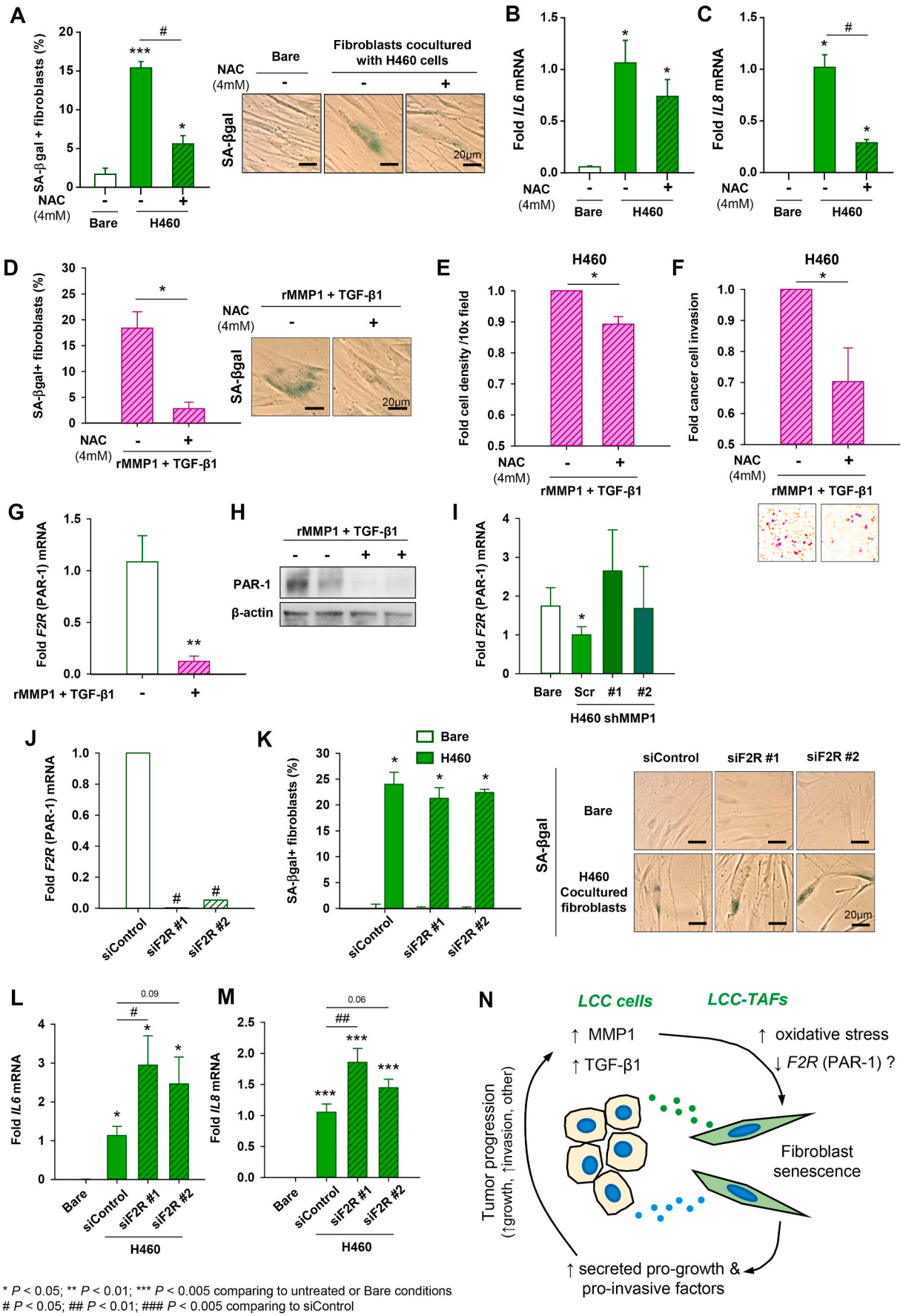

* $P < 0.05$; ** $P < 0.01$; *** $P < 0.005$ comparing to untreated or Bare conditions
\# $P < 0.05$; ## $P < 0.01$; ### $P < 0.005$ comparing to siControl

(caption on next page)

Fig. 6. Mechanistic insights underlying the pro-senescence and tumor-promoting effects caused by rMMP1 and TGF-β1 in fibroblasts. **A-C,** Senescent phenotype of fibroblasts cocultured alone (Bare) or with H460 cells with or without 4 mM of the antioxidant NAC in terms of percentage of SA-βgal+ cells (A) and mRNA expression of IL6 (B) and IL8 (C). **D,** Percentage of SA-βgal+ fibroblasts stimulated with 45U/ml rMMP1 and 2.5 ng/ml TGF-β1 with or without 4 mM of the antioxidant NAC as in Fig. 5A. **E and F,** Fold cell number density (E) and invasion (F) of H460 LCC cells stimulated with the CM obtained from fibroblasts cultured as in (D) and subsequently kept at serum-free medium for 4 days. **G-I,** Fold *F2R* (PAR-1) mRNA and protein expression of fibroblasts untreated or treated with rMMP1 and TGF-β1 as in Fig. 6D (G and H, respectively), or cocultured Bare or with H460 cells as in Fig. 1F (I). **J,** *F2R* (PAR-1) mRNA expression of fibroblasts upon *F2R* knock-down by siRNA for 48 h compared to siControl. **K,** Percentage of SA-βgal+ fibroblasts upon 48 h of *F2R* knock-down followed by coculture with LCC cells as in Fig. 1F. **L and M,** Fold *IL6* (L) and *IL8* (M) mRNA expression of fibroblasts upon *F2R* knock-down by siRNA for 48 h followed by coculture with control (Scr) H460 cells or Bare conditions for 5 days. **N,** Working model of the aberrant crosstalk between cells and fibroblasts in LCC. *, $P < 0.05$; **, $P < 0.01$; ***, $P < 0.005$ comparing to either untreated or Bare conditions. #, $P < 0.05$; ##, $P < 0.01$; ###, $P < 0.005$ comparing to siControl. Error bars indicate mean ± s.e.m. Mean values correspond to n ≥ 2 experiments.

fibroblasts cocultured with all these LCC lines, whereas it strongly abrogated the transcription of the ubiquitous pro-inflammatory SASP factors *IL6* and *IL8* in fibroblasts in one LCC line only. These results discourage a direct implication of IL6 and IL8 in the enhanced cancer cell growth and invasion elicited by the secretome of senescent fibroblasts in LCC. However, previous work supports the possibility that IL6 may contribute to LCC progression indirectly through a feedforward mechanism of fibroblast senescence amplification through sustained MMP1 upregulation in LCC cells, since IL6 upregulated MMP1 in lung cancer cells through increased STAT3 activation [19], and the IL6-rich conditioned medium of senescent fibroblasts enhanced STAT3 activation in lung cancer cells [41].

Broad-spectrum inhibition of MMPs has proven detrimental in cancer therapy, due in part to inhibition of necessary reparative functions [33]. Alternatively, our results support the exciting possibility of impairing the tumor-promoting traits of senescent TAFs in LCC and possibly other cancer types rich in senescent TAFs by directly removing them or inhibiting their aberrant secretome with senolytic and senostatic drugs, respectively [8]. Furthermore, our findings identify an *in vitro* preclinical model for testing potential therapies in LCC based on the coculture of pulmonary control fibroblasts with LCC cells, since it provides a straightforward supply of LCC-relevant senescent fibroblasts, thereby overcoming the intrinsic expansion limitations of cultured primary LCC-TAFs due to their enrichment in growth arrested cells through senescence as well as to the overall low incidence of LCC.

In summary, our results support that LCC cells elicit a tumor-supporting niche through the aberrant secretion of MMP1 and TGF-β1 to induce senescence in adjacent fibroblasts. Such aberrant increase in senescent TAFs may underlie, at least in part, the aggressive nature of LCC, since senescent fibroblasts enhanced the growth and invasion of LCC cells beyond those elicited by non-senescent fibroblasts, thereby raising the exciting possibility of testing anti-senescence drugs in future studies of this orphan disease.

Author contribution section

Conceptualization: Luca Roz, Derek Radisky and Jordi Alcaraz; **Data curation:** Marselina Arshakyan, Maria Maqueda and Alexandre Perera; **Formal analysis**: Marta Gabasa, Luca Roz, Derek Radisky, Evette Radisky and Jordi Alcaraz; **Funding acquisition:** Luca Roz, Noemí Reguart, Evette Radisky and Jordi Alcaraz; **Investigation:** Marta Gabasa, Rafael Ikemori, Giulia Bertolini, Alexandra Hockla, Paula Duch, Ornella Rondinone and Alejandro Llorente; **Methodology:** Marta Gabasa, Rafael Ikemori, Elena Gavilán, Albert Davalos, Josep Ramírez, Giulia Bertolini, Alexandra Hockla, Paula Duch, Alejandro Llorente, Marselina Arshakyan and Maria Maqueda; **Project administration:** Marta Gabasa, Luca Roz, Derek Radisky, Evette Radisky and Jordi Alcaraz; **Resources:** Luca Roz, Derek Radisky, Evette Radisky, Pere Gascón and Jordi Alcaraz; **Software:** Marselina Arshakyan, Maria Maqueda and Alexandre Perera; **Supervision:** Luca Roz, Derek Radisky and Jordi Alcaraz; **Validation:** Josep Ramírez, Noemí Reguart and Pere Gascón; **Visualization:** Marta Gabasa, Luca Roz, Derek Radisky and Jordi Alcaraz; **Roles/Writing – original draft:** Marta Gabasa, Luca Roz, Derek Radisky and Jordi Alcaraz; **Writing – review & editing:** Marselina Arshakyan, Alejandro Llorente, Paula Duch, Pere Gascón.

Declaration of competing interest

The authors declare that they have no conflict of interest.

Acknowledgements

We thank Sara Ozcoz, Raquel Bermudo, Èlia Alcañiz, Núria de la Iglesia (IDIBAPS), Federica Facchinetti and Giuliana Pollaci (IRCCS) and Elisabet Urrea (UB) for technical assistance, Manuel Serrano (IRB), Hidetoshi Mori (UC Davis) and Joan Montero (IBEC) for helpful discussions, and Daniel Navajas and Ramon Farré (UB) for support. This work was further supported by grants from the Agencia Estatal de Investigación (AEI/FEDER) (PI13/02368, SAF2016-79527-R and PID2019-110944RB-I00 (AEI/ 10.13039/501100011033) to JA, PI16/00890 to NR), Fundació Privada Cellex (to JA), National Institutes of Health (grant R01 GM132100 to ER), Generalitat de Catalunya (AGAUR SGR661 and CERCA Programme to JA), Junta Provincial de Barcelona de l'Associació Espanyola Contra el Càncer (AECC-B16-917 to JA), Italian Ministry of Health (RF-2016-02362946 to LR), Italian Association for Cancer Research (AIRC-IG21431 to LR), Sociedad Española de Neumología y Cirugía Torácica – SEPAR (SEPAR 437 to NR), COST Action (PROTEOSTASIS BM1307), and by fellowships from Ciência sem Fronteiras CNPq (to RI), and Universitat de Barcelona/beca APIF (to PD).

Appendix A. Supplementary data

Supplementary data to this article can be found online at https://doi.org/10.1016/j.canlet.2021.01.028.

References

[1] R.L. Siegel, K.D. Miller, A. Jemal, Cancer statistics, 2018, CA A Cancer J. Clin. 68 (2018) 7–30.

[2] W.D. Travis, E. Brambilla, A.G. Nicholson, Y. Yatabe, J.H.M. Austin, M.B. Beasley, L.R. Chirieac, S. Dacic, E. Duhig, D.B. Flieder, K. Geisinger, F.R. Hirsch, Y. Ishikawa, K.M. Kerr, M. Noguchi, G. Pelosi, C.A. Powell, M.S. Tsao, I. Wistuba, W.H.O. Panel, The 2015 world Health organization classification of lung tumors impact of genetic, clinical and radiologic advances since the 2004 classification, J. Thorac. Oncol. 10 (2015) 1243–1260.

[3] V. Mittal, T. El Rayes, N. Narula, T.E. McGraw, N.K. Altorki, M.H. Barcellos-Hoff, The microenvironment of lung cancer and therapeutic implications, in: A. Ahmad, S.M. Gadgeel (Eds.) Lung Cancer and Personalized Medicine: Novel Therapies and Clinical Management2016, pp. 75-110.

[4] J. Alcaraz, J.L. Carrasco, L. Millares, I.-C. Luis, F.J. Fernández-Porras, A. Martínez-Romero, N. Díaz-Valdivia, J. Sánchez De Cos, R. Rami-Porta, L. Seijo, J. Ramírez, M.J. Pajares, N. Reguart, E. Barreiro, E. Monsó, Stromal markers of activated tumor associated fibroblasts predict poor survival and are associated with necrosis in non-small cell lung cancer, Lung Canc. 135 (2019) 151–160.

[5] M. Puig, R. Lugo, M. Gabasa, A. Gimenez, A. Velasquez, R. Galgoczy, J. Ramirez, A. Gomez-Caro, O. Busnadiego, F. Rodriguez-Pascual, P. Gascon, N. Reguart, J. Alcaraz, Matrix stiffening and beta(1) integrin drive subtype-specific fibroblast accumulation in lung cancer, Mol. Canc. Res. 13 (2015) 161–173.

[6] R. Ikemori, M. Gabasa, P. Duch, M. Vizoso, P. Bragado, M. Arshakyan, I.C. Luis, A. Marin, S. Moran, M. Castro, G. Fuster, S. Gea-Sorli, T. Jauset, L. Soucek, L. M. Montuenga, M. Esteller, E. Monso, V.I. Peinado, P. Gascon, C. Fillat, F. Hilberg, N. Reguart, J. Alcaraz, Epigenetic SMAD3 repression in tumor-associated

fibroblasts impairs fibrosis and response to the antifibrotic drug nintedanib in lung squamous cell carcinoma, Canc. Res. 80 (2020) 276–290.
[7] D. Lambrechts, E. Wauters, B. Boeckx, S. Aibar, D. Nittner, O. Burton, A. Bassez, H. Decaluwe, A. Pircher, K. Van den Eynde, B. Weynand, E. Verbeken, P. De Leyn, A. Liston, J. Vansteenkiste, P. Carmeliet, S. Aerts, B. Thienpont, Phenotype molding of stromal cells in the lung tumor microenvironment, Nat. Med. 24 (2018) 1277.
[8] D. Munoz-Espin, M. Serrano, Cellular senescence: from physiology to pathology, Nat. Rev. Mol. Cell Biol. 15 (2014) 482–496.
[9] N. Basisty, A. Kale, O.H. Jeon, C. Kuehnemann, T. Payne, C. Rao, A. Holtz, S. Shah, V. Sharma, L. Ferrucci, J. Campisi, B. Schilling, A proteomic atlas of senescence-associated secretomes for aging biomarker development, PLoS Biol. 18 (2020), e3000599.
[10] Y. Hassona, N. Cirillo, K.P. Lim, A. Herman, M. Mellone, G.J. Thomas, G. N. Pitiyage, E.K. Parkinson, S.S. Prime, Progression of genotype-specific oral cancer leads to senescence of cancer-associated fibroblasts and is mediated by oxidative stress and TGF-beta, Carcinogenesis 34 (2013) 1286–1295.
[11] C. Capparelli, C. Guido, D. Whitaker-Menezes, G. Bonuccelli, R. Balliet, T. G. Pestell, A.F. Goldberg, R.G. Pestell, A. Howell, S. Sneddon, R. Birbe, A. Tsirigos, U. Martinez-Outschoorn, F. Sotgia, M.P. Lisanti, Autophagy and senescence in cancer-associated fibroblasts metabolically supports tumor growth and metastasis, via glycolysis and ketone production, Cell Cycle 11 (2012) 2285–2302.
[12] V. Paradis, N. Youssef, D. Dargere, N. Ba, F. Bonvoust, J. Deschatrette, P. Bedossa, Replicative senescence in normal liver, chronic hepatitis C, and hepatocellular carcinomas, Hum. Pathol. 32 (2001) 327–332.
[13] G. Yang, D.G. Roser, Z. Zhang, R.C. Bast Jr., G.B. Mills, J.A. Colacino, I. Mercado-Uribe, J. Liu, The chemokine growth-regulated oncogene 1 (Gro-1) links RAS signaling to the senescence of stromal fibroblasts and ovarian tumorigenesis, Proc. Natl. Acad. Sci. U. S. A 103 (2006) 16472–16477.
[14] T. Wang, F. Notta, R. Navab, J. Joseph, E. Ibrahimov, J. Xu, C.Q. Zhu, A. Borgida, S. Gallinger, M.S. Tsao, Senescent carcinoma-associated fibroblasts upregulate IL8 to enhance prometastatic phenotypes, Mol. Canc. Res. 15 (2017) 3–14.
[15] A. Chatterjee, S. Jana, S. Chatterjee, L.M. Wastall, G. Mandal, N. Nargis, H. Roy, T. A. Hughes, A. Bhattacharyya, MicroRNA-222 reprogrammed cancer-associated fibroblasts enhance growth and metastasis of breast cancer, Br. J. Canc. 121 (2019) 679–689.
[16] Y.H. Sun, S.W. Lin, C.C. Hsieh, Y.C. Yeh, C.C. Tu, K.J. Chen, Treatment outcomes of patients with different subtypes of large cell carcinoma of the lung, Ann. Thorac. Surg. 98 (2014) 1013–1019.
[17] R. Lugo, M. Gabasa, F. Andriani, F. Puig, F. Facchinetti, J. Ramírez, A. Gómez-Caro, U. Pastorino, G. Fuster, I. Almendros, P. Gascón, A. Davalos, N. Reguart, L. Roz, J. Alcaraz, Heterotypic paracrine signaling drives fibroblast senescence and tumor progression of large cell carcinoma of the lung, Oncotarget 7 (2016) 82324–82337.
[18] A. Weissferdt, Large cell carcinoma of lung: on the verge of extinction? Semin. Diagn. Pathol. 31 (2014) 278–288.
[19] N. Merchant, G.P. Nagaraju, B. Rajitha, S. Lammata, K.K. Jella, Z.S. Buchwald, S. S. Lakka, A.N. Ali, Matrix metalloproteinases: their functional role in lung cancer, Carcinogenesis 38 (2017) 766–780.
[20] M. Fanjul-Fernandez, A.R. Folgueras, A. Fueyo, M. Balbin, M.F. Suarez, M. Soledad Fernandez-Garcia, S.D. Shapiro, J.M.P. Freije, C. Lopez-Otin, Matrix metalloproteinase mmp-1a is dispensable for normal growth and fertility in mice and promotes lung cancer progression by modulating inflammatory responses, J. Biol. Chem. 288 (2013) 14647–14656.
[21] M.A. Cichon, V.G. Gainullin, Y. Zhang, D.C. Radisky, Growth of lung cancer cells in three-dimensional microenvironments reveals key features of tumor malignancy, Integr. Biol. 4 (2012) 440–448.
[22] Z. Yu, R. Visse, M. Inouye, H. Nagase, B. Brodsky, Defining requirements for collagenase cleavage in collagen type III using a bacterial collagen system, J. Biol. Chem. 287 (2012) 22988–22997.
[23] J. Batra, J. Robinson, A.S. Soares, A.P. Fields, D.C. Radisky, E.S. Radisky, Matrix metalloproteinase-10 (MMP-10) interaction with tissue inhibitors of metalloproteinases TIMP-1 and TIMP-2: binding studies and crystal structure, J. Biol. Chem. 287 (2012) 15935–15946.
[24] H. Ma, A. Hockla, C. Mehner, M. Coban, N. Papo, D.C. Radisky, E.S. Radisky, PRSS3/Mesotrypsin and kallikrein-related peptidase 5 are associated with poor prognosis and contribute to tumor cell invasion and growth in lung adenocarcinoma, Sci. Rep. 9 (2019) 1844.
[25] E. Piek, U. Westermark, M. Kastemar, C.H. Heldin, E.J. van Zoelen, M. Nister, P. Ten Dijke, Expression of transforming-growth-factor (TGF)-beta receptors and Smad proteins in glioblastoma cell lines with distinct responses to TGF-beta1, Int. J. Canc. 80 (1999) 756–763.
[26] K. Evangelou, N. Lougiakis, S.V. Rizou, A. Kotsinas, D. Kletsas, D. Munoz-Espin, N. G. Kastrinakis, N. Pouli, P. Marakos, P. Townsend, M. Serrano, J. Bartek, V. G. Gorgoulis, Robust, universal biomarker assay to detect senescent cells in biological specimens, Aging Cell 16 (2017) 192–197.
[27] M.D. Abramoff, P.J. Magelhaes, S.J. Ram, Image processing with ImageJ, Biophot. Int. 11 (2004) 36–42.
[28] M. Gabasa, R. Ikemori, F. Hilberg, N. Reguart, J. Alcaraz, Nintedanib selectively inhibits the activation and tumor-promoting effects of fibroblasts from lung adenocarcinoma patients, Br. J. Canc. 117 (2017) 1128–1138.
[29] J. Botling, K. Edlund, M. Lohr, B. Hellwig, L. Holmberg, M. Lambe, A. Berglund, S. Ekman, M. Bergqvist, F. Pontén, A. König, O. Fernandes, M. Karlsson, G. Helenius, C. Karlsson, J. Rahnenführer, J.G. Hengstler, P. Micke, Biomarker discovery in non-small cell lung cancer: integrating gene expression profiling, meta-analysis, and tissue microarray validation, Clin. Canc. Res. 19 (2013) 194–204.
[30] C.J. Scotton, R.C. Chambers, Molecular targets in pulmonary fibrosis - the myofibroblast in focus, Chest 132 (2007) 1311–1321.
[31] W. Sterlacci, D. Wolf, S. Savic, W. Hilbe, T. Schmid, H. Jamnig, M. Fiegl, A. Tzankov, High transforming growth factor beta expression represents an important prognostic parameter for surgically resected non-small cell lung cancer, Hum. Pathol. 43 (2012) 339–349.
[32] P. Arora, T.K. Ricks, J. Trejo, Protease-activated receptor signalling, endocytic sorting and dysregulation in cancer, J. Cell Sci. 120 (2007) 921–928.
[33] K. Kessenbrock, V. Plaks, Z. Werb, Matrix metalloproteinases: regulators of the tumor microenvironment, Cell 141 (2010) 52–67.
[34] M.L. Stallings-Mann, J. Waldmann, Y. Zhang, E. Miller, M.L. Gauthier, D. W. Visscher, G.P. Downey, E.S. Radisky, A.P. Fields, D.C. Radisky, Matrix metalloproteinase induction of Rac1b, a key effector of lung cancer progression, Sci. Transl. Med. 4 (2012), 142ra195.
[35] J. D'Armiento, T. DiColandrea, S.S. Dalal, Y. Okada, M.T. Huang, A.H. Conney, K. Chada, Collagenase expression in transgenic mouse skin causes hyperkeratosis and acanthosis and increases susceptibility to tumorigenesis, Mol. Cell Biol. 15 (1995) 5732–5739.
[36] B. Hinz, Myofibroblasts, Exp. Eye Res. 142 (2016) 56–70.
[37] L.L. da Motta, M.A. De Bastiani, F. Stapenhorst, F. Klamt, Oxidative stress associates with aggressiveness in lung large-cell carcinoma, Tumour Biol. : J. Int. Soc. Oncodevelop. Biol. Med. 36 (2015) 4681–4688.
[38] G.J. Fisher, T. Quan, T. Purohit, Y. Shao, M.K. Cho, T. He, J. Varani, S. Kang, J. J. Voorhees, Collagen fragmentation promotes oxidative stress and elevates matrix metalloproteinase-1 in fibroblasts in aged human skin, Am. J. Pathol. 174 (2009) 101–114.
[39] J. Iida, J.B. McCarthy, Expression of collagenase-1 (MMP-1) promotes melanoma growth through the generation of active transforming growth factor-beta, Melanoma Res. 17 (2007) 205–213.
[40] M.K. Ruhland, A.J. Loza, A.H. Capietto, X. Luo, B.L. Knolhoff, K.C. Flanagan, B. A. Belt, E. Alspach, K. Leahy, J. Luo, A. Schaffer, J.R. Edwards, G. Longmore, R. Faccio, D.G. DeNardo, S.A. Stewart, Stromal senescence establishes an immunosuppressive microenvironment that drives tumorigenesis, Nat. Commun. 7 (2016) 11762.
[41] B. Chen, Y. Liang, L. Chen, Y. Wei, Y. Li, W. Zhao, J. Wu, Overexpression of klotho inhibits HELF fibroblasts SASP-related protumoral effects on non-small cell lung cancer cells, J. Canc. 9 (2018) 1248–1258.